NJC

Accepted Manuscript

This is an *Accepted Manuscript*, which has been through the Royal Society of Chemistry peer review process and has been accepted for publication.

Accepted Manuscripts are published online shortly after acceptance, before technical editing, formatting and proof reading. Using this free service, authors can make their results available to the community, in citable form, before we publish the edited article. We will replace this *Accepted Manuscript* with the edited and formatted *Advance Article* as soon as it is available.

You can find more information about *Accepted Manuscripts* in the Information for Authors.

Please note that technical editing may introduce minor changes to the text and/or graphics, which may alter content. The journal's standard Terms & Conditions and the Ethical guidelines still apply. In no event shall the Royal Society of Chemistry be held responsible for any errors or omissions in this *Accepted Manuscript* or any consequences arising from the use of any information it contains.

ROYAL SOCIETY OF CHEMISTRY

www.rsc.org/njc

Tailoring the Structure and Electronic Properties of Platinum and Gold-Platinum Nanocatalysts Towards Enhanced O_2 Activation.

Krati Joshi and Sailaja Krishnamurty
Functional Materials Division, CSIR-Central Electrochemical Research Institute, Karaikudi-630 006, India

Geometric structure plays a crucial role in enhancing the catalytic activity of a material towards reactions such as oxygen reduction, methanol oxidation etc. Pt and Pt based bimetallic alloys of different morphologies such as nanorods, core-shell etc. have been synthesized so far contributing to varying catalytic activity in fuel cells. However, the electronic factors contributing to enhanced catalytic activity of a particular structure/shape/morphology are not understood so far. In a first such computational study, we demonstrate this complex structure-property correlation on model six atom Pt clusters in the context of O_2 activation at cathode material of direct methanol fuel cells. Since, recent studies have shown that Au-Pt bimetallic alloys exhibit superior catalytic activity towards oxygen reduction reaction with respect to other bimetallic clusters, we have identified 4 distinct six atom Pt cluster morphologies: viz., triangular planar, distorted octahedral, normal octahedral and double square planar and doped them sequentially with gold atoms till a ratio of 1:1 is obtained. Thus, clusters with varying conformations/shapes and bimetallic compositions are considered for potential O_2 activation. The O-O bond stretching frequencies, are calculated to evaluate the degree of bond activation in O_2 molecule. Our study reveals that the Pt_6 and Au_nPt_m (n+m=6) clusters with a double square planar shape exhibit superior catalytic activity towards O-O bond activation with respect to other six atom conformations. Analysis of their electronic properties demonstrates that, the amount of charge transferred by cluster to the O_2 molecule and the effective overlap between the d-orbitals of metal atom and pi molecular orbitals of O_2 can be directly correlated with their catalytic activities. In order to validate these conclusions, we have further extended such analysis on various Pt_m (m = 3-13) conformations, where, once again the frontier molecular orbital composition is seen to play a predominant role in oxygen activation. Thus, the present study unveils the electronic properties determining the catalytic activity of a catalytic cluster towards O-O bond activation.

Keywords: Catalytic Activity, O_2 Activation, Pt Clusters, Au-Pt Bimetallic Clusters, Density Functional Theory, Red shift in O_2 stretch frequency.

I. INTRODUCTION.

Direct Methanol Fuel Cells (DMFC) are growingly attractive on account of their high energy density and biodegradability.[1] In spite of being one of the most environment friendly cells, the technology of DMF cells has not taken off due to the disadvantages associated with commonly used 2-8 nm sized Pt nanoparticles[2] which act as electro-catalysts at both cathode and anode. It is now widely accepted that Pt based electro-catalysts are not selective towards both methanol oxidation reaction at anode and Oxygen Reduction Reaction (ORR) at cathode.[3] To overcome this overwhelming disadvantage, several research works have been devoted in designing better catalysts for cathode and anode by alloying Pt nanoclusters with other d-block elements such as Ni, Pd, Rh, Ru, Co, Au etc.[4–9] It is generally observed that alloying leads to catalysts that are more active for ORR and simultaneously tolerant to methanol at cathode.

Interestingly, most of the alloys suffer from base dissolution or are less efficient as compared to Pt catalysts with few exceptions such as Au:[10] (a) Au being a noble metal like Pt, stabilizes the alloy, thereby, leading to a more attractive and efficient catalyst.[11–14] (b) Au having higher oxidation potential than Pt, alloys of Pt with Au have shown better ORR activity as compared to that of pure Pt catalyst.[15,16] It is also believed that the presence of Au reduces the CO poisoning of the catalyst.[11,12,17] (c) Au-Pt nanocatalysts are reported to have greater methanol tolerance at the cathode in the case of DMFCs compared to the pure Pt nanocatalysts.[10,18–20]

However, the major hurdle associated in the effective practical application of Au-Pt or even other nanoalloy clusters in fuel cells[14,19,21,22] is the lack of perception on precise electronic factors contributing to their enhanced electro-catalytic activity. Factors such as synthesis conditions, support and preparation route,[23–29] contribute to alloy formation with varying structural effects (core-shell, random, multishell, ordered, disordered, graded structures etc.). These structural/morphological effects in turn play a paramount role in controlling its catalytic activity.

In spite of availability of many advanced experimental methodologies (such as selective leaching, multi-step synthesis etc.) that assist in controlling the surfaces of nanoparticles, a precise correlation between the structure/morphology and catalytic activity within bimetallic clusters in the context of DMFCs is elusive. This has motivated many theoretical researchers to address structure-activity-stability correlation in Au-Pt clusters.[30–45] However, interestingly, though Au-Pt nanoalloys are known for their excellent ORR activity, most of the studies on have been devoted to analyze their catalytic activity by CO adsorption. Few recent combined experimental and

theoretical studies have demonstrated that ORR activity of Au-Pt can be enhanced by the ensemble effect of surface Au atoms.[46,47] In another work, Nazari et al[48] have theoretically investigated the ORR activity of CNT supported Au-Pt bimetallic nanoclusters. They found that, the supported Au-Pt clusters show improved catalytic activity towards ORR. However, supported clusters are thermodynamic unstable with respect to their bare counterparts.[48] Thus, theoretical investigations addressing specifically ORR activity of Au-Pt or even that of Pt clusters are limited and investigations correlating structure- electronic property- ORR activity are unavailable.

In this context, in the present work we have studied the catalytic activity of Pt and Au-Pt alloy clusters towards O_2 molecule. For this purpose we have chosen a six atom Pt cluster. We analyze the catalytic activity as a function of its various isomers following which, we extend the studies to six atom Au-Pt clusters with three different atomic compositions (Au_nPt_m, n:m = 1:5, 2:4, 3:3) viz., Au_1Pt_5, Au_2Pt_4, and Au_3Pt_3. Thus, the activation of O_2 molecule on Au-Pt alloy clusters is evaluated as a function of varying shape and composition. In the present work, the catalytic activity of a given structure towards O_2 molecule is analyzed in terms of activation of O_2 molecule on these six atom clusters.

A number of studies have shown that, ORR on platinum based catalysts proceeds through a direct 4 electron conversion of oxygen to water.[49] This mechanism involves formation of various intermediates such as OH, OOH etc.[50,51] In connection with this mechanism, O-O bond breaking is the most critical step. The first step in the O-O bond breaking mechanism is the activation of the oxygen molecule which invariably controls the activation barrier in ORR.[52] The extent of activation can be measured or understood from the increase in O_2 bond length, amount of charge transferred to the oxygen molecule and most importantly extent of red shift in the stretching frequency of the molecule. Based on these three parameters, it is theoretically possible to identify the electro-catalytic ability of a catalyst towards oxygen reduction reaction.

We would like to note that the present study is also significant to some extent from the experimental point of view. During the last 3-4 years, there have been serious attempts to further reduce the size of Pt based nanocatalysts below 1 nm due to understandable advantages from the catalytic and economic point of view. Reduced size results in an increase of the surface area and thereby higher catalytic activity. Small sized particles lower considerably the cost of the catalyst in Pt based systems. Remarkable advances have been made in this area in recent years[53–61] where researchers have succeeded in reducing the nanoparticle size to less than 1 nm. In fact, due to availability of advanced techniques such as Atomic Layer Deposition (ALD) single Pt atom catalyst fabrication on supports has been achieved.[57] In several other cases, the cluster sizes with less than 100 atoms have been synthesized and applied at catalysts.[59–62] In a more recent work, researchers have reported experimental results where Pt_{12} cluster is more catalytically active as compared to the icosahedral Pt_{13} clusters. In short, in the size range of 2-100 atoms, the shape and bimetallic composition is likely to play a predominant role in the oxygen reduction reaction mechanism. Our study clearly brings out the important and fundamental correlation between the shape-electronic structure-activation property of an atomic cluster in this size range.

II. COMPUTATIONAL DETAILS

All calculations are performed in the framework of Density Functional Theory (DFT), using a linear combination of Gaussian orbitals as implemented in the Gaussian 09[63] code. Several conformations are generated for Pt_6 clusters and optimized using Perdew-Burke-Ernzerhof (PBE)[64] exchange and correlation functional under default convergence criterion with Berny algorithm. LANL2DZ basis set and the corresponding Los Alamos relativistic effective core potential (RECP)[65] is used to take into account scalar relativistic effects for platinum atoms. Following the geometry optimization, harmonic vibrational frequencies are computed for various conformations. All the frequencies are found to be positive thereby, indicating them to be a local minima. The geometries are compared with the lowest energy conformations of Pt_6 cluster reported in the literature (see Figure 1).

Five sample conformations among the ten noted structures are considered for further study of O_2 activation. The basis for choosing these conformations is discussed in the next section. O_2 molecule is adsorbed on various atomic sites of the chosen clusters. The cluster-O_2 complexes are optimized using the same functional as mentioned above. After optimization, the activation of the O_2 molecule in the complex is analyzed following the computation of harmonic frequencies of the optimized complexes. TZVP[66] basis set is used for oxygen atoms.

Following the analysis of the catalytic activity of model Pt_6 conformations, the chosen conformations are sequentially doped Au atoms till the bimetallic ratio reaches 1:1 thereby generating Au_nPt_m (n:m = 1:5, 2:4, 3:3) clusters. O_2 molecule is adsorbed on various atomic sites of these bimetallic clusters and the complexes are optimized. LANL2DZ basis set is used for Au and Pt atoms during these calculations and O atoms are treated with DZVP basis set as in earlier cases. Once again the adsorption energies and activation of O_2 molecule by Au_nPt_m clusters are analyzed.

The binding energy or adsorption energy of O_2 on different Pt_6 and Au_nPt_m clusters is calculated using the following formula :

$$B.E. = E_C - (E_L + E_M) \quad (1)$$

where, B.E. is the binding energy of O_2 with the metal

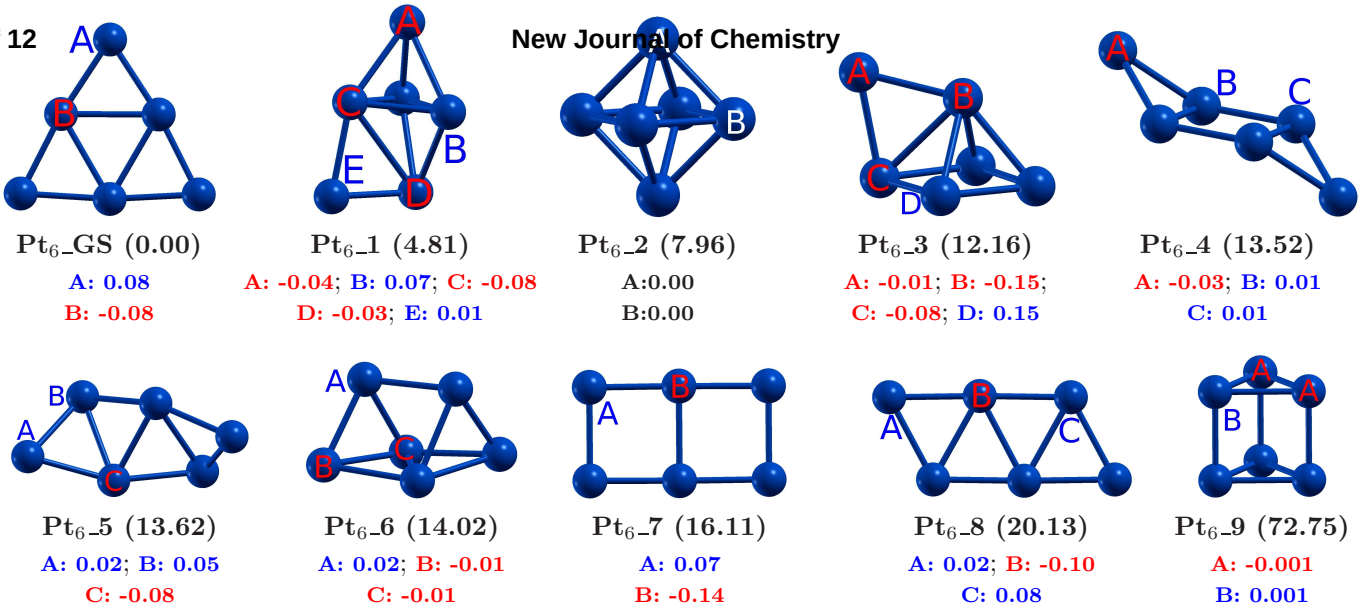

Pt_6_GS (0.00)
A: 0.08
B: -0.08

Pt_6_1 (4.81)
A: -0.04; B: 0.07; C: -0.08
D: -0.03; E: 0.01

Pt_6_2 (7.96)
A:0.00
B:0.00

Pt_6_3 (12.16)
A: -0.01; B: -0.15;
C: -0.08; D: 0.15

Pt_6_4 (13.52)
A: -0.03; B: 0.01
C: 0.01

Pt_6_5 (13.62)
A: 0.02; B: 0.05
C: -0.08

Pt_6_6 (14.02)
A: 0.02; B: -0.01
C: -0.01

Pt_6_7 (16.11)
A: 0.07
B: -0.14

Pt_6_8 (20.13)
A: 0.02; B: -0.10
C: 0.08

Pt_6_9 (72.75)
A: -0.001
B: 0.001

Fig. 1

Putative models of Pt_6 clusters. The relative energies (kcal/mol) are given in the parenthesis. Given below the figures are NPA derived charges (e) on various chemically distinct sites. Red colour represents negatively charged sites and blue colour represents positively charged sites.

clusters. E_C is the energy of the relaxed O_2-metal cluster complex and E_L is the energy of O_2. E_M is the energy of metal cluster (Pt_6 and Au_nPt_m). Natural Bonding Orbital (NBO) analysis is also performed and all the Frontier Molecular Orbitals (FMOs) are plotted at an iso-surface value of 0.01.

III. RESULTS AND DISCUSSIONS

A. Putative models of Pt_6 clusters and their nomenclature.

Various possible conformations of Pt_6 are shown in Figure 1. The relative energy of each conformation is given in the parenthesis. Chemically different sites in each conformation are marked as A, B, C, D, etc. as shown in Figure 1. Charges on these sites as obtained by natural population analysis are given below the Figure. Positively charged centers are represented by blue colour and negatively charged centers are represented in red colour. We note that the above conformations may be classified based on (a) dimensionality (2D/3d), (b) symmetry and charge distribution. Pt_6_GS, Pt_2, Pt_4, Pt_6 and Pt_9 are symmetric non-planar conformations where all the atoms are in nearly neutral state. In other words, as understood from NPA population analysis, there is very little charge redistribution within the cluster. Pt_{GS}, Pt_7 and Pt_8 are planar conformations showing moderate charge redistribution, while rest of the conformations are non-planar conformations with C1 symmetry. The non-planar conformations with C1 symmetry show maximum polarized distribution of atomic charges within the cluster.

Among the Pt_6 conformations discussed above, we choose the following representative conformations for further studies: (a) Three planar conformations, viz., Pt_{GS}, Pt_7 and Pt_8 as planar conformations are well known for their catalytic activity. (b) One non-symmetric 3D structure, viz., Pt_1. (c) One symmetric 3D structure (octahedral), viz., Pt_2. Out of the chosen conformations: (a) Pt_6_GS is the ground state structure, (b) Pt_6_1 and Pt_6_2 are low lying conformations and (c) Pt_6_7 and Pt_6_8 are high lying conformations.

Before proceeding further to dope these clusters with Au atoms to generate bimetallic clusters or before adsorbing O_2 molecule on these conformations, it is important to ensure that these conformations are thermodynamically stable at room temperatures. Several high energy conformations convert into another minima at finite temperatures. Hence, the possibility of the structure retaining its shape at finite temperatures is analyzed using Born-Oppenheimer Molecular Dynamical (BOMD) simulations. Each of the above discussed conformations is subjected to BOMD simulations at 350 K. BOMD simulations are performed with deMon2k[67] software suit using DFT for about 50 picoseconds under NVT ensemble. Velocity-verlet algorithm is used to scale time and Nose-Hoover thermostat[68,69] is used to maintain the temperature constant. It is interesting to note that all the five chosen conformations retain their structure at 350 K. This is demonstrated by plotting the bond length fluctuations within these clusters as a function of time in Supporting information Figure 1 (supp-fig.1). Following

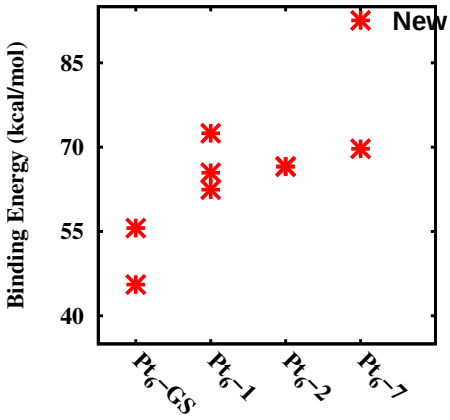

Fig. 2
Binding Energies (kcal/mol) of O_2 molecule with various Pt_6 conformations.

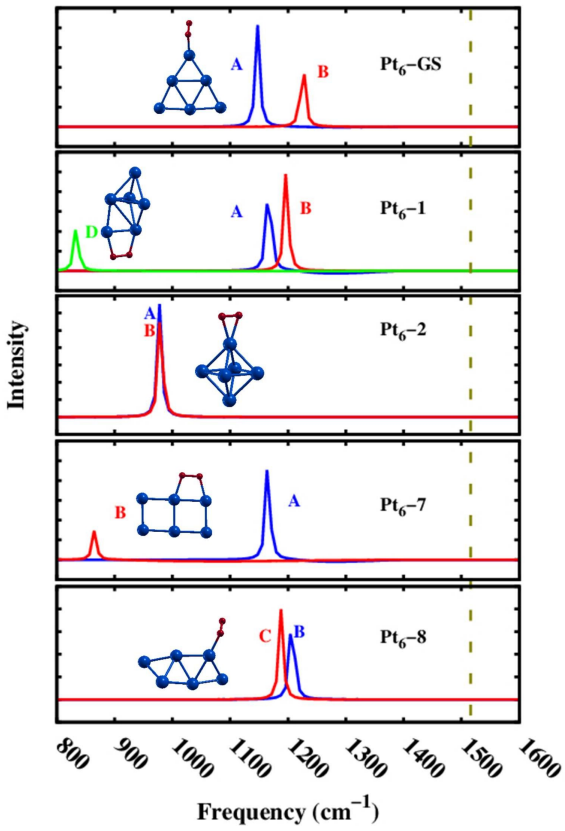

Fig. 3
IR stretching frequencies (cm^{-1} of O-O bond in various Pt_6–O_2 complexes. The dotted line represents the O-O stretching frequency of gas phase O_2 molecule. Different colored peaks correspond to different adsorption sites available in a given conformation.

the conformation of their thermodynamic stability, chemical stability of these conformations is also conformed as some of the conformations undergo structural modifications after adsorption of supports such as graphene of carbon nanotubes.[48]

B. O_2 activation on Pt_6 clusters as a function of shape.

As already mentioned, the principal aim of this study is to investigate the O_2 activation as a function of the shape of catalyst. Hence, O_2 is adsorbed at chemically different sites on five Pt_6 isomers discussed above and the complexes are optimized under the conditions mentioned in the computational details section. It is well established that, O_2 binds to metal clusters in three distinct ways: (1) Both oxygen atoms bond with one metal atom, Griffith mode, (2) Terminal O_2 binds via a single bond to metal atom, Pauling mode and (3) O_2 forms a bridge between two metal atoms, (Yeager or bridge mode).[48] All the above mentioned binding modes of O_2 are observed on the metal clusters used in the current study, especially Pauling and Yeager mode. The binding energy of O_2 with various Pt_6 conformations is given in Figure 2. Although there is no clear trend noted in case of the binding energy, the binding energy is greater in case of high lying conformations.

Next we analyze the shift in the IR stretch frequency of O-O bond in the metal-O_2 complexes with respect to that in bare O_2 molecule. We note that the O-O stretching frequency of isolated O_2 molecule is 1512 cm^{-1} and in line with previous theoretical studies.[71] The changes in the stretching frequencies upon adsorption on any structure is a measure of activation of the molecule and this is a well established case in the literature.[72,73] It is also noteworthy to mention here that earlier, Fielicke et al[74] have experimentally investigated the activation of molecular oxygen on anionic gold clusters by using Infrared Multiple-Photon Dissociation (IR-MPD) spectroscopy as a probe. They have demonstrated the formation of superoxo species (O_2^-) on gold cluster surfaces with a O-O stretching frequency around 1060 cm^{-1}.

O-O stretching frequencies in various Pt_6–O_2 complexes are given in the Figure 3. The corresponding optimized geometries are highlighted in the same figure. It is observed that on Pt_6_1 (D-site) and Pt_6_7 (B-site) conformations oxygen bonds via bridging or Yeager mode. On the other hand, oxygen shows Pauling and Griffith type of bonding modes upon adsorption on Pt_6-GS, Pt_6-8 and Pt_6-2 conformations, respectively. Noticeably, the longest O-O bond distances of 1.38 Å, 1.37 Å and 1.36 Å are observed on Pt_6_1 (D-site) and Pt_6_7 (B-site) and Pt_6_2 clusters respectively. On the other hand, O-O bond is least affected on Pt_6_GS (1.29 Å) and Pt_6_8 (1.27 Å) conformations. It should be noted that O-O bond length of gas phase O_2 molecule is 1.22 Å which is in well agreement with the values reported

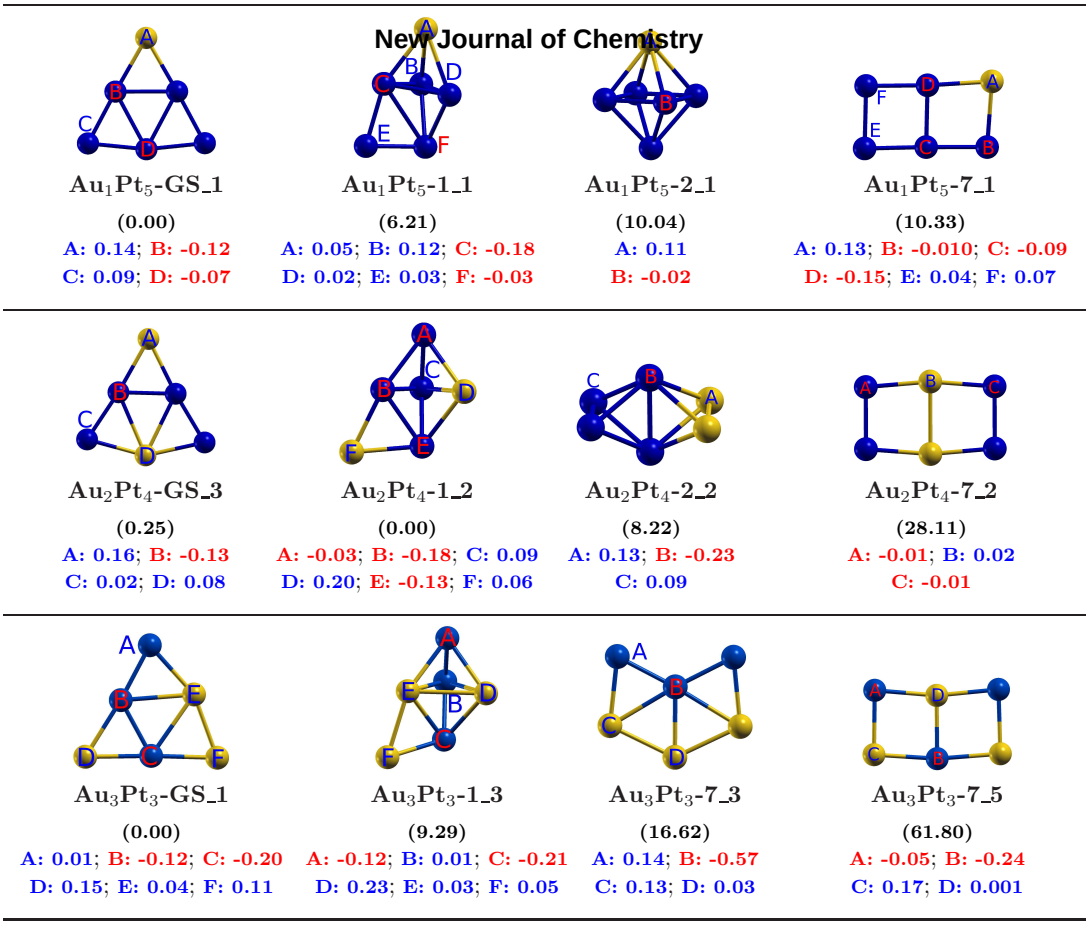

Fig. 4

Putative models of six atom Au_nPt_m (n,m = 1,5; 2,4; 3,3) clusters. The relative energies (kcal/mol) are given in the parenthesis. Given below the figures are NPA derived charges (e) on chemically distinct sites. Red colour represents negatively charged sites and blue colour represents positively charged sites.

by earlier groups.[75] The O-O bond length fluctuations observed on Pt_6 conformations as a function of shape can be corroborated by examining the O-O IR stretching frequency, which is given in the Figure 3. To our expectations, maximum red-shifts (of about 700-750 cm^{-1}) in the O-O stretching frequency with respect to isolated oxygen molecule is observed for the double square planar Pt_6_7 (B-Site) and non-planar Pt_6_1 (D-Site) (distorted octahedral) conformations as compared to the other conformations. The next highest fluctuation in O-O bond stretching frequency ($\sim 600cm^{-1}$) is observed in the case of octahedral Pt_6_2 conformation. As expected the O-O bond stretching frequency in case of triangular planar Pt_6_GS and zig-zig Pt_6_8 conformations is least affected. The above results have revealed some alluring facts about the activation of oxygen molecule on the platinum clusters. Noticeably, although O_2 molecule is adsorbed on all the available adsorption sites on different Pt_m conformations, only few sites are able to activate O_2. For example, double square planar Pt_6_7 have two distinct adsorption sites A and B (see Figure 1), however O_2 is activated only when it is adsorbed on B-site. Another interesting fact about oxygen activation on Pt_6 clusters is that, bridging or Yeager mode is the most activated type of O_2 bonding mode (Pt_6_7, Pt_6_1) as compared to other two bonding modes. This is consistent with the earlier reports, which states that O_2 is most activated in peroxo form then the superoxo form.[76] The most interesting understanding emerging out from the present study is that, oxygen molecule exhibits enhanced activation on specific Pt_6 conformations (Pt_6_7 and Pt_6_1). It is noteworthy, that earlier experimental reports have highlighted the fact that catalytic properties[77] of platinum nano-clusters (with sizes ranging from 3 nm-20 nm) are shape/morphology dependent.

C. Putative models of six atom Au_n-Pt_m (n+m=6) clusters and their nomenclature.

Out of the five Pt_6 conformations studied in the earlier section, four most catalytically active ones (Pt_{GS},

Pt_1, Pt_2 and Pt_7) are used as precursors for generating several Au-Pt bimetallic conformations. We emphasize here that the main aim of the present study is to study the morphology-catalytic activity correlation in Au_nPt_m alloy clusters and not to find out the global minimas of these clusters. Hence, the bimetallic conformations are generated by doping the above mentioned four precursor Pt_6 conformations with 1, 2 and 3 Au atoms at various possible sites resulting into three different bimetallic alloy compositions: viz, Au_1Pt_5, Au_2Pt_4 and Au_3Pt_3. Au_nPt_m conformations are named after their precursor Pt_6 conformations. For example, the conformations which are generated from Pt_6_GS, Pt_6_1, Pt_6_2 and Pt_6_7 are named as Au_nPt_m-GS_k, Au_nPt_m-1_k, Au_nPt_m-2_k and Au_nPt_m-7_k respectively, where k = 1, 2, 3, 4 etc.

Owing to the availability of multiple atomic rearrangements, number of isomers increases with the number of Au atoms for a Au_nPt_m bimetallic cluster. For instance, in case of Au_1Pt_5, Pt_6_GS can be doped with single Au atom in two different ways to give two Au_1Pt_5-GS conformations (triangular planar). Similarly, for the cases of Au_2Pt_4 and Au_3Pt_3, doping of Pt_6_GS with 2 and 3 Au atoms results in three and six Au_2Pt_4-GS and Au_3Pt_3-GS conformations respectively. Similar method is adopted to generate Au_nPt_m conformations of other shapes as well (Pt_6_1, Pt_6_2 and Pt_6_7). As a result, there are 8 Au_1Pt_5, 12 Au_2Pt_4 and 15 Au_3Pt_3 conformations which makes a total of 35 Au_nPt_m conformations. It is not possible to show the geometries of all 35 Au_nPt_m conformations in one figure therefore, one representative conformation of each shape (GS, 1, 2 and 7) from all the three Au_nPt_m compositions are presented in the Figure 4.

Similar to the case of Pt_6 conformations (see Figure 1) the energies, NPA derived charges and adsorption sites are highlighted for different Au_nPt_m conformations in the Figure 4. The geometries of remaining Au_nPt_m isomers are given in supp-fig.2 of supporting information. The ground state geometry of Au_1Pt_5 and Au_3Pt_3 is same as that of Pt_6. However, for Au_2Pt_4 binary system, two degenerate isomers (Au_2Pt_4-GS_3 and Au_2Pt_4-1_2) are available as its possible ground state conformations.

D. O_2 activation by Au_nPt_m alloy clusters as a function of shape and composition.

O_2 molecule is adsorbed on various chemically distinct adsorption sites (both Pt and Au) of various Au_nPt_m alloy clusters discussed above (see Figure 4) and the geometries are optimized. The final optimized geometries are given in the supporting information (see supp-fig.3). O_2 molecule bonds via Pauling or Yeager mode with all the Au_nPt_m alloy clusters as in case of Pt_6 conformations. The binding energies (kcal/mol) of O_2 molecule with Au_nPt_m alloy clusters is plotted as a function of shape and composition and is given in the supporting information (see supp-fig.4). It is observed that, binding energies of O_2 with Au_nPt_m-GS_k, Au_nPt_m-1_k, Au_nPt_m-7_k conformations is lower than 40 kcal/mol. It may be recalled that the corresponding values on Pt_6 counterpart conformations is greater than 55 kcal/mol. Exceptions to this are some of the Au_3Pt_3-7_k conformations which have almost equal binding energies with O_2 molecule as that of Pt_6-7 cluster (see area highlighted in red arrow

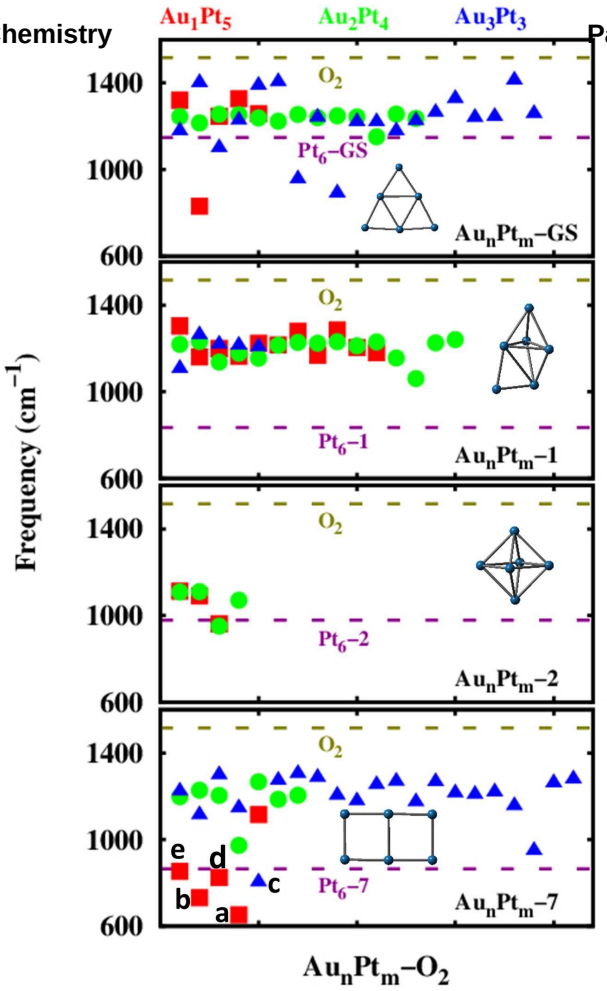

Fig. 5

O-O vibrational stretching frequencies (cm^{-1}) on Au_nPt_m clusters as a function of shape and composition. Green and violet dotted lines in the graph corresponds to the O-O stretching frequency in isolated O_2 molecule and the lowest O-O stretching frequency observed in corresponding parent Pt_6–O_2 complex. Red squares represent stretch frequencies in Au_1Pt_5–O_2 complexes. Green spheres represent stretch frequencies on Au_2Pt_4–O_2 complexes. Blue triangles represent stretch frequencies on Au_3Pt_3–O_2 complexes. Label a is Au_1Pt_5-7_2 (C-site, 652 cm^{-1}, b is Au_1Pt_5-7_1 (E-site, 732 cm^{-1}) c is Au_3Pt_3-7_2 (B-site 800 cm^{-1}), d is Au_1Pt_5-7_2 (E-Site, 825 cm^{-1}), e is Au_1Pt_5-7_1 (D-Site, 853 cm^{-1}).

in supp-fig.4). It may be recalled that this cluster (Pt_6-7) and Pt_6-1 are the most catalytically active clusters. Au_nPt_m-2_k–O_2 (conformations with octahedral shape) conformations are unstable with positive binding energies (plot is not shown).

Next, we analyze the activation of O_2 molecule on various Au_nPt_m alloy clusters of different shapes and compositions. Figure 5 gives the O_2 stretching frequency for various Au_nPt_m compositions and shapes. Most visible point is that there are very few Au-Pt conformations which activate O_2 molecule better than its corresponding Pt clusters. Salient observations from Figure 5 plots are as follows:

(a) Visibly, the Au-Pt conformations derived from distorted octahedral conformation, (Pt_6-1, cluster which shows maximum O-O activation) are less effective in activating the O-O bond with respect to its Pt_6 analog (See second plot in Figure 5).

(b) Same is the case with Au_nPt_m-2 conformations, structures derived from octahedral Pt clusters. However, two Au-Pt conformers with n,m = 1,5 and 2,4 show marginal improved activation with respect to their Pt analog structure (See third plot in Figure 5). However, the corresponding O_2 adsorbed complexes are unstable as evidenced from their positive O_2 binding energies (see the discussion in the above paragraph).

(c) Some of the Au-Pt conformations derived from Triangular planar geometry show enhanced O_2 bond activation (signified by lower IR stretch frequency of O-O bond in the complex. These are: (i) Au_1Pt_5-GS_1 (D-Site, Figure 4) and (ii) Au_3Pt_3-GS_2 (B, D Sites, see supporting information). The O-O stretching frequencies in the above three cases are 830 cm^{-1}, 890cm^{-1} and 950 cm^{-1}, respectively (See first plot in Figure 5). The corresponding O-O bond lengths for Au_1Pt_5-GS_1 (D-Site) and Au_3Pt_3-GS_2 (B and D Sites) conformations are 1.37 Å, 1.36 Å and 1.34 Å, respectively. These O-O stretching frequencies are thus 200-350 cm^{-1} times lower then that of triangular planar Pt_6-GS conformations. On the other hand, none of the triangular planar conformations of Au_2Pt_4 bimetallic composition are efficient in activating O-O bond.

(d) Figure 5 further reveals that the double square planar Au_1Pt_5-7_1 (E and D site), Au_1Pt_5-7_2 (E and C sites) and Au_3Pt_3-7_2 (B-site) are exceptionally efficient in activating O-O bond with stretching frequencies of 732 cm^{-1}, 853 cm^{-1}, 825 cm^{-1}, 652 cm^{-1}, and 800 cm^{-1} respectively (for geometries, see supporting information). The longest O-O bond length is seen in case of Au_1Pt_5-7–O_2 complex (O-O stretch frequency of 652 cm^{-1}) is 1.50 Å. This is higher then the value reported in one of the recent study on Au-Pt alloy, where O-O bond is activated up to a distance of only 1.42 Å.[48] On the other hand, the performance of Au_2Pt_4-7_k bimetallic alloys (double

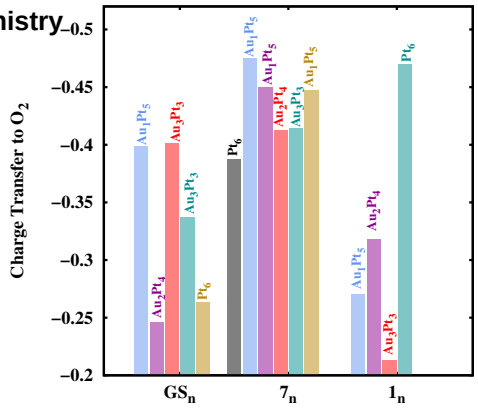

Fig. 6
Comparison of the charge transferred (e) by Pt_m and Au_nPt_m clusters to the adsorbed O_2 molecule as a function of conformation.

square planar towards O_2 molecule activation is poor. It may be recalled that the Pt_6-7 structure (double square planar) is more efficient in activating O_2 molecule with respect to other conformations.

In short, the above observations indicate that, among four different shapes of conformations studied in the present investigation, alloying the double square planar and triangular (Pt_6) conformations with Au atoms results in enhanced activation of O_2 molecule. On the other hand, alloying the distorted octahedral conformation (Pt_6_2) conformation does not result in enhanced O_2 activation. Such kind of behavior indicates that, the activation of O_2 molecule by Au_nPt_n and Pt_6 systems is a highly conformation dependent process. Among three different Au-Pt bimetallic compositions in six atom clusters, based on of their performance, Au-Pt compositions can be systematically ordered as: $Au_1Pt_5 \geq Au_3Pt_3 > Au_2Pt_4$

It may be noted that experimental studies[61,78,79] demonstrated varying Au-Pt compositions such as 2:1,[80,81] $Au_{22}Pt_{78}$[28] or even 1:1[29] exhibit extraordinary electrocatalytic activity towards ORR. The present study demonstrates that composition plays a predominant role in enhancing the catalytic activity of the parent Pt structure.

E. Charge transfer and molecular orbital composition: Correlation to the O_2 activation ability.

The present investigation has put forward several interesting facts about the oxygen activation by Pt_6 and Au_nPt_m (n+m=6) clusters. As we have already seen, properties such as the shape or morphology, the chemical composition of the catalyst (Pt_6 and Au_nPt_m) are playing a decisive role in the activation of oxygen. To decipher, how these properties are influencing the O_2 ac-

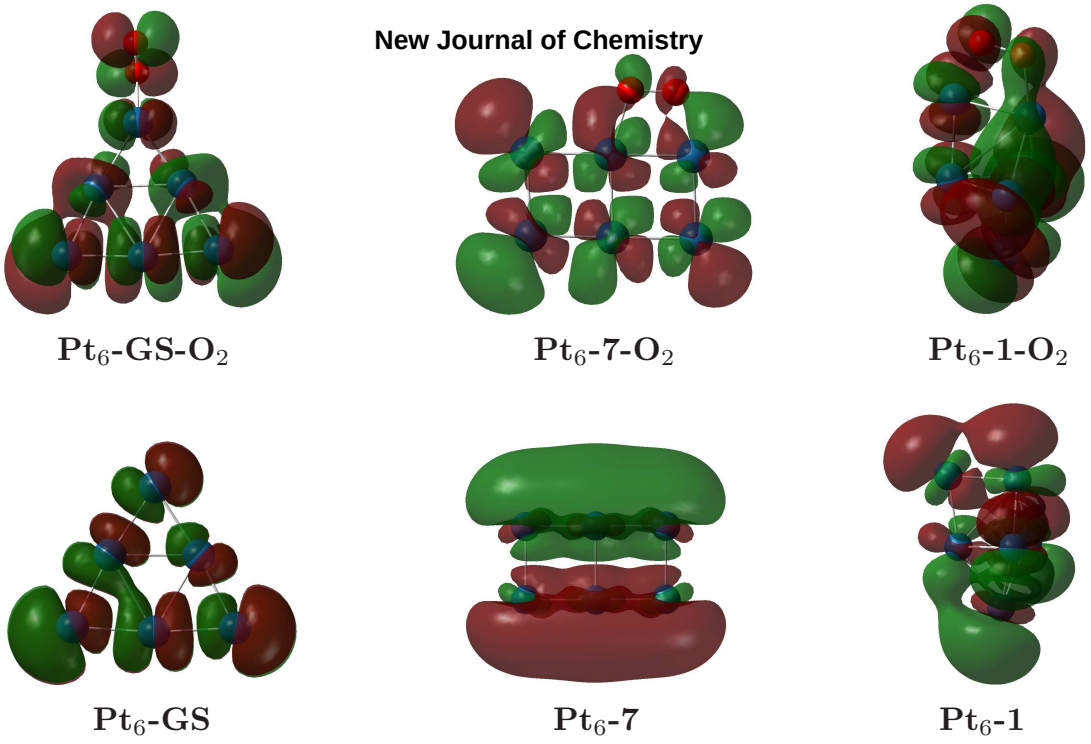

Fig. 7
Highest Occupied Molecular Orbitals (HOMOs) of Pt_6 clusters and O_2–Pt_6 complexes.

tivation, a thorough analysis of their electronic structure is mandatory. For this purpose, first we have evaluated the net amount of charge (NPA) transfer occurring between the adsorbed oxygen molecule and the cluster (Pt_m and Au_nPt_m) as a function of shape. The plot of charge transferred to O_2 molecule as a function of shape for Pt_m and Au_nPt_m clusters is presented in the Figure 6. As already seen, in case of Pt_6 clusters, the Pt_6-1 conformations with distorted octahedral shape show maximum activity towards O-O bond activation, whereas triangular planar Pt_6-GS conformations are performing poor. On the other hand, in case of Au_nPt_m alloy clusters, the double square planar Au_1Pt_5-7_k conformations are are more active, whereas, Au_nPt_m-1 conformations (distorted octahedral) are performing poor towards O-O bond activation. This can be correlated with the amount of charge transferred by these clusters to the adsorbed oxygen. From Figure 6, it is clear that a significant amount of charge (0.47e, 0.46e) is transferred by the most active Au_1Pt_5-7_2 and Pt_6-1 clusters to the adsorbed oxygen molecule. In contrast, least active Au_nPt_m-1_k and Pt_6-GS conformations show a lower amount of charge transfer (0.21-0.32e). It should be noted that, the amount of charge transferred by the cluster to the adsorbed oxygen results in excess electron density in the O_2 $2\pi^*$ antibonding molecular orbital. As a consequence, O-O bond length increases. This is in well agreement with the earlier reports which states that, the charge transfer to the O_2 molecule plays a predominant role in O-O bond elongation.[48]

Moreover, in general it is observed that the clusters with double square planar conformation (7_n) are able to facilitate more charge transfer to adsorbed O_2 molecule as compared to clusters of other conformations (GS_n, 1_n). As a result, former is performing better towards O_2 activation as compared to later. The performance of Au_nPt_m clusters with different conformations increases in the order 1_n (distorted octahedral) < GS_n (triangular planar) < 7_n (double square planar).

To understand the underlying electronic factors contributing to the enhanced activation of O_2 by double square planar conformations, Highest Occupied Molecular Orbitals (HOMOs) of Pt_6-GS, Pt_6-7 and Pt_6-1 conformations are presented in the Figure 7. The HOMO of Pt_6-GS shows that, its triangular planar conformation is not efficient to facilitate an easy overlap between the metal d-orbital of the cluster and π-orbitals of O_2 molecule. As a result, there is a negligible amount of charge transfer between the adsorbed O_2 molecule and the cluster and hence O-O bond remains unaffected. In contrast to it, the Pt_6-7 (double square planar) and Pt_6-1 (distorted octahedral) are facilitating an easy and strong overlap between the metal d-orbitals and the O_2 π-orbitals. In particular, HOMO of conformation with double square planar structure shows presence of continuous distribution of electron density around the cluster. Consequently, the adsorbed O_2 molecule abstracts significant amount of charge from the cluster and gets

activated. The above observations indicate that, for the activation of O_2 molecule, the Au_nPt_m and Pt_m based nanocatalysts should be designed in such a way that their conformation allows an easy and strong overlap between metal d-orbitals and O_2 π-orbitals.

To validate the above observations, we have further carried out calculations on Pt_m (m=3-13) clusters of different conformations and sizes. Different conformations of Pt_3, Pt_4, Pt_5, Pt_7, Pt_8, Pt_9, Pt_{12} and Pt_{13} clusters are generated. The HOMOs of these conformations are presented in the supporting information (supp-fig5). From these results it is observed that among different Pt_m clusters (m = 3-13), only Pt_3, Pt_9 and Pt_{12} conformations have a de-localized HOMO. These conformations show consistently longer O-O bond lengths when O_2 molecules are adsorbed on these three clusters as compared to rest of the clusters. For example, in case of Pt_3 clusters, conformation with linear conformation has a de-localized HOMO, while the triangular Pt_3 conformation has a localized HOMO. O-O bond length when complexes with linear Pt_3 cluster is 1.44$\mathring{A}$. On the other hand while when O_2 molecule complexes with triangular cluster its corresponding bond length is 1.36 $\mathring{A}$. Another notable comparison is between Pt_{12} and Pt_{13} clusters: The HOMO of Pt_{12} cluster is more de-localized as compared to that of icosahedron conformation Pt_{13} cluster. This is consistent with the results reported in one of the recent experimental study where Pt_{12} cluster is observed to be electrochemically more active then the icosahedral Pt_{13} cluster.[61] Above results indicates that, our theoretical findings are not specific to six atom clusters and are valid for other larger sized clusters as well.

IV. CONCLUSIONS

The present work brings out the structure dependent catalytic activity of Pt and Au-Pt clusters. Earlier works have brought out the size sensitivity. However, a clear correlation of structure dependent catalytic behavior of atomic clusters in the context of ORR was missing in the literature so far. In the first computational study of its kind, we have investigated the O_2 molecule activation as a function of conformation and composition of Pt_m and Au_nPt_m clusters. A confluence of structure-morphology and electronic factors contribute to the catalytic activity of Pt_m and Au_nPt_m clusters concerning O_2 activation. The reasons contributing towards exceptionally high activity of a nanocluster towards O_2 activation can be corroborated from their electronic properties:

(i) The amount of charge transferred from cluster to the adsorbed oxygen molecule is playing a dominant role in O-O bond weakening. Maximum charge transfer (0.47e) between cluster and oxygen is observed in case of Pt_m and Au_nPt_m double square planar clusters.

(ii) Among the three possible O_2 bonding modes viz. Griffith, Pauling and Yeager mode, the later two modes are mostly observed on Pt_m and Au_nPt_m clusters. However, the O-O bond is most activated when O_2 is bonded to cluster in Yeager or bridge mode.

(iii) For the first time, a detailed and systematic analysis of electronic properties of clusters and its influence in determining its catalytic activity is discussed. The clusters with more de-localized HOMO orbitals exhibit better oxygen activation as compared to the ones exhibiting localized HOMO density. FMO analysis shows that, clusters with double square planar structures have de-localized HOMO density around itself. Consequently, they are capable of allowing a stress and strain-free effective overlap between metal d-orbitals and pi orbitals of oxygen molecule. As a result more amount of charge can be transferred from cluster to the oxygen, which in turn leads to the enhanced catalytic activity of Pt_m and Au_nPt_m clusters (Double Square planar shape) towards O-O bond activation. Such kind of electronic effect is also observed in Pt_m cluster of different sizes. Pt_3, Pt_9, Pt_{12} conformations of a particular shape are also observed to have a de-localized HOMO density, which is indicative that our findings are not specific to six atom cluster and are consistent among clusters of larger sizes as well.

(iv) Significantly, earlier works have reported that only Pt adsorption sites in a bimetallic clusters such as Au-Pt, Ru-Pt participate in the oxygen reduction mechanism. In the above present study, we have explored both Au and Pt adsorption sites for ORR. While the study shows that O_2 molecule preferable adsorbs on Pt atoms, the study further reveals that Au sites can participate in an active way during the activation of the oxygen molecule. For example, in case of Au_1Pt_5-7_1 (D-Site) and Au_1Pt_5-7_2 (E-Site) (see Supporting information Figure 3), oxygen molecule is bridged (Yeager mode) between one Au and one Pt adsorption site.

(v) The study reveals that doping by Au atoms does not always lead to enhanced O_2 activation. Activation can be enhanced for only particular shapes and sizes and Au:Pt compositions. In case of a six atom cluster, the relative activity of different Au_nPt_m compositions can be arranged in the following order: Au_1Pt_5 >> Au_3Pt_3 >> Au_2Pt_4

In short, our study demonstrates that, the catalytic activity of an electro-catalyst towards O_2 activation is intrinsically coupled to the extent of localization/de-localization within its frontier molecular orbitals. This activation can be further enhanced by tuning the electronic properties as a function of shape, doping and extent of doping. As already mentioned, higher activation of O_2 molecule is indicative of a lower activation barrier towards the formation of stable intermediates such as OH, OOH etc. during oxygen reduction reaction. This criterion can be used theoretically to effectively identify or choose an electro-catalyst for performing ORR particularly for clusters with atoms below 100 atoms. Above the this size range, surface/morphology/shape sensitive

electronic properties (frontier molecular orbital properties) are likely to converge to single crystal limit when the number of atoms in the cluster are greater than 147.[82]

V. ADDRESS FOR CORRESPONDENCE

Sailaja Krishnamurty, e-mail: sailaja.raaj@gmail.com
Krati Joshi, e-mail: krati.joshi81@gmail.com

VI. ACKNOWLEDGMENTS

The authors acknowledge the Center of Excellence in Computational Chemistry (COESC) at CSIR-NCL, Pune and CSIR-Fourth Paradigm Institute, Bangalore for providing access to their high performance computing facilities. Authors acknowledge a grant from MSM: CSC-0129 project. Authors acknowledge Mohammed Azeezulla Nazrulla for helpful discussions. The authors greatly acknowledge one of the reviewers whose comments have helped us to put in the entire work in a more organized manner.

[1] A.S. Arico, S. Srinivasan, V.Antonucci, *Fuel Cells.*, 2001, **1**, 133-161.
[2] B.C. Steele, A. Heinzel, *Nature,* 2001, **414**, 345-352.
[3] K. Scott, A. K. Shukla, *Modern Aspects of Electrochemistry*, 2007, **40**, 127-227.
[4] H. Liu, C. Song, L. Zhang, J. Zhang, H. Wang, D. P. Wilkinson, *J. Power Sources*, 2006, **155**, 95-110.
[5] E. Antolini, T. Lopes, E. R. Gonzalez, *J. Alloys Compd.*, 2008, **461**, 253-262.
[6] J. L. Fernandez, V. Raghveer, A. Manthiram, A. J. Bard, *J. Am. Chem. Soc.*, 2005, **127**, 13100-13101.
[7] T. Toda, H. Igarashi, H. Uchida, M. Watanabe, *J. Electrochem. Soc.*, 1999, **146**, 3750-3756.
[8] J. N Tiwari, R. N. Tiwari, G. Singh, K. S. Kim, *Nano Energy*, 2013, **2**, 553-578.
[9] B. Lim, M. Jiang,P. H. C. Camargo, E.C. Cho, J. Tao, X. Lu, Y. Zhu,Y. Xia, *Science*, 2009, **324**, 1302-1305.
[10] G. Selvarani, S. V. Selvaganesh, S. Krishnamurthy, G.V.M. Kiruthika, P. Sridhar, S. Pitchumani, A. K. Shukla, *J. Phys. Chem. C*, 2009, **113**, 7461-7468.
[11] J. Suntivich, Z. Xu, C. E. Carlton, J. Kim, B. Han,S. W. Lee, N. Bonnet, N. Marzari, L. F. Allard, H. A. Gasteiger, K. Hamad-Schifferli, S. Shao-Horn, *J. Am. Chem. Soc.*, 2013, **135**, 7985-7991.
[12] S. Boopathi, S. Senthil Kumar, *J. Phys. Chem. C*, 2014, **118**, 29866-29873.
[13] J. B. Xu, T. S. Zhao, W. W. Yang, S. Y. Shen, *Int. J. Hydrogen Energy*, 2010, **35**, 8699-8706.
[14] J. Luo, M. M. Maye, N. N. Kariuki, L. Wang, P. N. Njoki, L. Han, M. Schadt, Y. Lin, H. R. Naslund, C. J. Zhong, *Catal. Today.*, 2005, **99**, 291-297.
[15] J. Zhang, K. Sasaki, E. Sutter, R. R. Adzic, *Science*, 2007, **315**, 220.
[16] Y. Zhang, Q. H. Huang, Z. Q. Zou, J. F. Yang, W. Vogel, H. J. Yang, *Phys. Chem. C*, 2010, **114**, 6860.
[17] J. Wang, G. Yin, G. Wang, Z. Wang, Y. Gao, *Electrochem. Comm.*, 2008, **10**, 831-834.
[18] N. Illayaraja,N. Prabhu, N. Lakshminarasimhan, P. Murugan, D. Jeyakumar, *J. Mater. Chem. A*, 2013, **1**, 4048-4056.
[19] P. Hernández-Fernández, S. Rojas, P. Ocón, A. de Frutos, J. M. Figueroa, P. Terreros, M. A. Pena, J. L. G. Fierro, *J. Power Sources*, 2008, **177**, 9-16.
[20] Y. B. Lou, M. M. Maye,L. Han, J. Luo,C. J. Zhong, *Chem. Commun.*, 2001, 473-474.
[21] C. Mihut, D. B. Chandler, M. D. Amirdis, *Catal. Commun.*, 2002, *3*, 91-97.
[22] S. Chilukuri, T. Joseph, S. Malwadkar, C. Damle, S. B. Halligudi,B. S. Rao, M. Sastry, P. Ratnasamy, *Stud. Surf. Sci. Catal.*, 2003, **146**, 573-576.
[23] J. Zhang, D. N. Oko, S. Garbarino, R. Imbeault, M. Chacker, A. C. Tavares, D. Guay, D. Ma, *J. Phys. Chem. C*, 2012, **116**, 13413-13420.
[24] K-S. Lee, H-Y. Park, H. C. Ham, S. J. Yoo, H. J. Kim, E. Cho, A. Manthiram, J. H. Jang, *J. Phys. Chem. C*, 2013, **117**, 9164-9170.
[25] H. Ataee-Esfahani, L. Wang, Y. Nemoto, Y. Yamauchi, *Chem. Mater.*, 2010, **22**, 6310-6318.
[26] B. D. Chandler,A. B. Schabel, C. F. Blanford, L. H. Pignolet, *J. Catal.*, 1999, **187**, 367-384.
[27] P. Hernández-Fernández, S. Rojas, P. Ocón, J. L. G. de la Fuente, J. S. Fabián, J. Sanza, M. A. Pena, F. J. GarcÍa-García, P. Terreros, J. L. G. Fierro, *J. Phys. Chem. C*, 2007, **111**, 2913-2923.
[28] H. You, F. Zhang, Z. Liu, J. Fang,*ACS Catal.*, 2014, **4**, 2829-2835.
[29] A. Guo, J. Li, S. Dong, E. Wang,*J. Phys. Chem. C*, 2010, **114**, 15337-15342.
[30] D. W. Yuan, Y. Wang, Z. Zeng, *J. Chem. Phys.*, 2005, **122**, 114310-114321.
[31] A. M. Asaduzzaman, M. Springborg, *Phys. Rev. B*, 2005, **72**, 165422.
[32] W. Q. Tian, M. Ge, F. Gu, T. Yamada, Y. Aoki, *J. Phys. Chem. A*, 2006, **110**, 6285-6293.
[33] W. Q. Tain, M. Ge, F. Gu, Y. Aoki, *J. Phys. Chem. A*, 2005, **109**, 9860-9866.
[34] L. Leppert, R. Q. Albuquerque, A. S. Foster, S. Kummel, *J. Phys. Chem. C*, 2013, **117**, 17268-17273.
[35] H. B. Liu, U. Pal, J. A. Ascencio, *J. Phys. Chem. C*, 2008, **112**, 19173-19177.
[36] L. Deng, W. Hu, H. Deng, S. Xiao, *J. Phys. Chem. C*, 2010, **114**, 11026-11032.
[37] N. Braidy, G. R. Purdy,G. A. Botton, *Acta Mater.*, 2008, **56**, 5972-5983.

[38] R. Esparza, J. A. Ascencio, G. Rosas, J. F. Sánchez Ramírez, U. Pal, R. Perez, *J Nanosci. Nanotechnol.*, 2005, **5**, 641-647.

[39] K. Koszinowski, D. Schroder, H. Schwarz, *ChemPhysChem*, 2003, **4**, 1233-1237.

[40] Q. Ge, C. Song, L. Wang, *Comput. Mater. Sci.*, 2006, **35**, 247-253.

[41] C. Song, Q. Ge, L. Wang, *J. Phys. Chem. B*, 2005, **109**, 22341-22350.

[42] M. M. Sadek, L. Wang, *J. Phys. Chem. A*, 2006, **110**, 14036-14042.

[43] O. Olvera-Neria, A. Cruz, H. Luna-Gracia, A. Anguiano-Gracia, E. Poulain, S. Castillo, *J. Chem. Phys.*, 2005, **123**, 164302-164308.

[44] J. H. Mokkath, U. Schwingenschlogl, *J. Phys. Chem. C*, 2013, **117**, 9275-9280.

[45] K. Mondal, A. Banerjee, T. K. Ghanty, *J. Phys. Chem. C.*, 2014, **118**, 11935-11945.

[46] Y. T. Liang, S. P. Lin, C. W. Liu, S. R. Chung, T. Y. Chen, J. H. Wang, K. W. Wang, *Chem. Comm.*, 2015, **51**, 6605.

[47] S. P. Lin, K. W. Wang, C. W. Liu, H. S. Chen, J. H. Wang, *J. Phys. Chem. C.*, 2015, **119**, 15224-15231.

[48] F. Shojaei, M. Mousavi, F. Nazari, F. Illas, *Phys. Chem. Chem. Phys.*, 2015, **17**, 3659-3672.

[49] Y. Nie, L. Li, Z. Wei, *Chem. Soc. Rev.*, 2015, **44**, 2168-2201.

[50] T. Zhang, A. B. Anderson, *Electrochimica Acta*, 2007, **53**, 982-989.

[51] A. B. Anderson, J. Roques, S. Mukerjee, V. S. Murti, N. M. Markovic, V. Staminkovic, *J. Phys. Chem. B*, 2005, **109**, 1198-1203.

[52] L. Zhang, Z. Xia, *J. Phys. Chem. C*, 2011, **115**, 11170-11176.

[53] B. Qiao et. al. *Natur. Chem*, 2011, **3**, 634.

[54] S. T. Christensen et. al. *Small*, 2009, **5**, 750.

[55] J. S. King, et al. *Nano Lett.*, 2008, **8**, 2405.

[56] C. Lui, C. C. Wang, C. C. Kei, Y. C. Hsueh, T. P. Perng, *Small*, 2009, **5** 1535-1538.

[57] S. Sun, G. Zhang, N. Gauquelin, N. Chen, J. Zhou, S. Yang, W. Chen, X. Meng, D. Geng, M. N. Banis, R. Li, S. Ye, S. Knights, G. A. Botton, T-K. Sham, X. Sun, *Scientific Reports*, 2013, **3**, 1775.

[58] E. Yoo, T. Okada, J. Akita, M. Kohyama, I. Honma, J. Nakumura, *J. Power Sources*, 2011, **196**, 110.

[59] Y. Shen, Z. Zhang, K. Xaio, J. Xi, *Phys. Chem. Chem. Phys.*, 2014, **16**, 21609.

[60] S. Mukherjee, B. Ramalingam, K. Gangopadhyay and S. Gangopadhyay, *J. Electro. Chem. Soc.*, 2014, **161**, F493.

[61] I. Takane, K. Hirokazu, C. Wang-Jae, O. Saori, A. Ken, Y. Kimihisao, *J. Am. Chem. Soc.*, 2013, **135**, 13089-13095.

[62] B. Fang, B. N. Wanjala , X. Hu, J. Last, R. Loukrakpam, J. Yin, J. Luo, C.-J. Zhong, *J. Pow. Sou.*, 2011, **196**, 659-665.

[63] **Gaussian 09, Revision A.1**, M. J. Frisch GWT, H. B. Schlegel, G. E. Scuseria, M. A. Robb, J. R. Cheeseman, G. Scalmani, V. Barone, B. Mennucci, G. A. Petersson, H. Nakatsuji, M. Caricato, X. Li, H. P. Hratchian, A. F. Izmaylov, J. Bloino, G. Zheng, J. L. Sonnenberg, M. Hada, M. Ehara, K. Toyota, R. Fukuda, J. Hasegawa, M. Ishida, T. Nakajima, Y. Honda, O. Kitao, H. Nakai, T. Vreven, J. A. Montgomery, Jr., J. E. Peralta, F. Ogliaro, M. Bearpark, J. J. Heyd, E. Brothers, K. N. Kudin, V. N. Staroverov, R. Kobayashi, J. Normand, K. Raghavachari, A. Rendell, J. C. Burant, S. S. Iyengar, J. Tomasi, M. Cossi, N. Rega, J. M. Millam, M. Klene, J. E. Knox, J. B. Cross, V. Bakken, C. Adamo, J. Jaramillo, R. Gomperts, R. E. Stratmann, O. Yazyev, A. J. Austin, R. Cammi, C. Pomelli, J. W. Ochterski, R. L. Martin, K. Morokuma, V. G. Zakrzewski, G. A. Voth, P. Salvador, J. J. Dannenberg, S. Dapprich, A. D. Daniels, . Farkas, J. B. Foresman, J. V. Ortiz, J. Cioslowski, and D. J. Fox., 2009. Gaussian, Inc, Wallingford CT

[64] J. P. Perdew, K. Burke, M. Ernzerhof, *Phy. Rev. Lett.*, 1996, **77**, 3865.

[65] P. J. Hay, W. R. Wadt, *J. Chem. Phys.*, 1985, **82**, 270-83.

[66] A. Schaefer, C. Huber, R. Ahlrichs, *J. Chem. Phys.*, 1994, **100**, 5829-5835.

[67] A. M. Koster, P. Calaminici, M. E. Casida, R. F-Moreno, G. Geudtner, A. Goursot, T. Heine, A. Ipatov, F. Janetzko, J. M. del Campo, S. Patchkovskii, J. U. Reveles, A. Vela, D. R. Salahub, deMon2k deMon Developers 2006.

[68] S. Nose, *J. Chem. Phys.*, 1984, **81**, 511.

[69] W.G. Hoover, *Phys. Rev. A*, 1985, **31**, 1695.

[70] Pt_6_GS, Pt_6_1, Pt_6_2 and Pt_6_7 conformations are seen to adsorb on a graphene nanoflake without any significant conformational modifications of distortions (see supp-fig. 6 for demonstration).

[71] K. Huber, G.herzberg, *Constants of Diatomic Molecules NIST Chemistry WebBook, NIST Standard Reference Database Number 69*, P. Linstrom, W. Mallard , National Institute of Standards and Technology.

[72] R. L. T. Parreira, S. E. Galembeck, *J. Mol. Struct. (THEOCHEM)*, 2006, **760**, 59-63.

[73] R. L. T. Parreira, S. E. Galembeck, P. Hobza, *ChemPhysChem*, 2007, **8**, 87-92.

[74] A. P. Woodham, G. Meijer, A. Fielicke, *Angew. Chem. Int. Ed.*, 2012, **51**, 4444-4447.

[75] D. H. Lim, J. Wilcox, *J. Phys. Chem. C*, 2011, **115**, 22742-22747.

[76] R. Pal, L. M. Wang, Y. Pei, L. S. Wang, X. C. Zeng, *J. Am. Chem. Soc.*, 2012, **134**, 9438-9445.

[77] W. Yu, M. D. Porosoff, J. G. Chen, *Chem. Rev.*, 2012, **112**, 5780-5817.

[78] T. Imaoka, H. Kitazawa, W.-J. Chun, S. Omura, K. Albrecht, K. Yamamoto, *J. Phys. Chem. C*, 2013, **117**, 26998-27006.

[79] J. S. Ratliff, S. A. Tenney, X. Hu, S. F. Conner, S. Ma, D. A. Chen, *Langmuir*, 2009, **25**, 216-225.

[80] S. Guo, L. Wang, S. Dong, E. Wang, *J. Phys. Chem. C*, 2008, **112**, 13510-13515.

[81] W. Ye ,H. Kou , Q. Liu, J. Yan, F. Zhou, C, Wang, *Int. J. Hyd. Ene.*, 2012, **37**, 4088-4097.
C. Chao Li, W. Zhang, H. Ang, H. Yu, B. Yu Xia, X. Wang, Y. Hui Yang, Y. Zhao, H. Hoon Hng, Q. Yan, *J. Mater. Chem. A*, 2014, **2**, 10676-10681.

[82] L. Li, A. H. Larsen, N. A. Romero, V. A. Morozov, C. Glinsvad, F. A-Pedersen, J. Greeley, K. W. Jacobsen, J. K. Norskov, *J. Phys. Chem. Lett.*, 2013 **4**, 222-226.

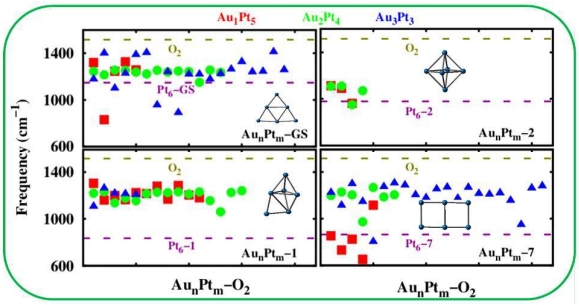

Structural design of precious metal molecular catalyst by doping is proved to significantly enhance its activity.